chemistry

MDPI

Article

Encryption Using Cholesteric Liquid Crystal Epoxy Film with Regionally Tailored Cross-Linking

Yingying Yi, Wenqian Yang, Yi Li, Wei Liu and Yonggang Yang *

State and Local Joint Engineering Laboratory for Novel Functional Polymeric Materials, Department of Polymer Science and Engineering, College of Chemistry, Chemical Engineering and Materials Science, Soochow University, Suzhou 215123, China; y717999@163.com (Y.Y.); 20224209250@stu.suda.edu.cn (W.Y.); liyi@suda.edu.cn (Y.L.); weiliu@suda.edu.cn (W.L.)

* Correspondence: ygyang@suda.edu.cn

Abstract

Vividly colored cholesteric liquid crystal polymer network (CLCN) patterns based on epoxy resin are used in decorative and anti-counterfeiting applications. These films are typically prepared via cationic photopolymerization and post-polymerization to achieve a high cross-linking degree. In this work, the cross-linking degree is controlled by varying the UV irradiation dosage during photopolymerization. Following this, the reflection band of the CLCN film changes after removing non-cross-linked compounds with acetone. Leveraging the low cationic polymerization rate and the chain termination capability of methanol, a structurally colored CLCN film with regionally tailored cross-linking was fabricated. With the treatment of acetone, a colorful pattern was observed. Moreover, upon immersion in methanol, the film swelled, revealing a colorful pattern. After the evaporation of methanol, the pattern disappeared. Consequently, this CLCN film holds significant potential for information encryption applications.

Keywords: cationic photopolymerization; cholesteric liquid crystal polymer network; cross-linking degree; structural color; epoxy resin

1. Introduction

As one-dimensional photonic crystal materials, cholesteric liquid crystals (CLCs) exhibit wavelength- and polarization-selective reflection due to their periodically helical superstructure, resulting in vibrant structural colors [1,2]. A standard preparation method involves doping nematic liquid crystals with chiral dopants [3–5]. By modulating chiral dopant concentration, the helical pitch can be tuned to precisely control the reflection wavelength. To stabilize these structural colors, reactive monomers are incorporated into the CLC mixture to form cross-linked cholesteric liquid crystal polymer networks (CLCNs) via photopolymerization [6,7]. This cross-linking process permanently fixes the helical architecture, thereby preserving its photonic properties. This strategy provides a robust platform for developing structurally colored coatings and solid-state photonic devices with long-term stability [8].

To date, polyacrylate-based CLCN films have been extensively studied and applied in fields such as decoration, anti-counterfeiting, sensors, and displays [9–25]. However, their preparation via radical polymerization is susceptible to oxygen inhibition, typically requiring fabrication within a confined cell or under an inert atmosphere. In contrast, epoxy resin-based CLCN films rely on cationic photopolymerization. This process is unaffected by

Check for updates

Academic Editor: Matthias Lehmann

Received: 17 January 2026
Revised: 10 February 2026
Accepted: 12 February 2026
Published: 13 February 2026

Copyright: © 2026 by the authors. Licensee MDPI, Basel, Switzerland. This article is an open access article distributed under the terms and conditions of the Creative Commons Attribution (CC BY) license.

oxygen interference, enabling efficient film fabrication directly in air [26,27]. The resulting cross-linked network imparts the films with excellent thermal stability, mechanical strength, chemical resistance, and high adhesive force on substrates [28–34]. Recently, structural color CLCN films have been fabricated using reactive epoxy liquid crystal monomers and chiral dopants. Their inherent patterning capability makes these films particularly suitable for decoration and anti-counterfeiting applications [34–36].

With the rapid increase in information technology, the importance of information security has become increasingly prominent, and numerous advanced strategies have been developed for information encryption and data protection [37,38]. Among these, a strategy that achieves dynamic information encryption by constructing regions with varying cross-linking degrees within polymer films has gradually emerged as a research hotspot. This approach utilizes controlled UV exposure during photopolymerization to create regions with distinct cross-linking degrees within the film. These regions exhibit differentiated swelling behaviors or optical responses under solvent, heat, or mechanical stimulation, enabling information concealment under normal conditions and revelation upon specific stimulation. This cross-linking degree-based encryption mechanism has been effectively validated in various functional polymer systems, demonstrating its universality and feasibility [39–41]. However, it is worth noting that existing encryption methods based on cross-linking degree regulation still have certain limitations: most rely on external energy inputs such as thermal fields, electric fields, or near-infrared light and thus impose specific requirements on operating environments and equipment; some systems achieve multi-response capabilities, their high costs hinder large-scale application; and certain methods still require mechanical stretching, high-temperature post-processing, or specialized encapsulation during the modulation process, limiting their practical application in simple, repeatable encryption scenarios. CLCN films exhibit unique optical tunability and stimulus-responsive potential due to their combination of the helical structure of CLCs and the elasticity of polymer networks [8]. Therefore, extending this strategy to CLCN films with superior processability and material stability holds promise for developing high-performance information encryption platforms.

To achieve the aforementioned cross-linking degree-regulated encryption strategy, precise control over the polymerization process is crucial. Photopolymerization has become a prevalent method for fabricating highly cross-linked polymer networks, owing to its room-temperature processability, low energy consumption, and minimal organic solvent emissions [42–47]. In the cationic polymerization of epoxy monomers, UV irradiation activates photoinitiators to generate strong acids, which initiate the ring-opening polymerization mechanism. Notably, the extended lifetime of cationic active centers allows polymerization to persist even after light exposure concludes—a phenomenon referred to as the "dark curing" or post-curing stage [48–53]. In polymerization systems, the presence of water or monohydric alcohols leads to chain transfer reactions [54]. Alcohols act as nucleophiles, attacking the positively charged end of the growing polymer chain and forming an ether bond. Monohydric alcohols serve as chain transfer agents, reacting with active centers to terminate polymerization, while dihydric alcohols function as cross-linking agents, participating in polymer network formation [55–58]. Herein, colorful epoxy resin-based CLCN films with tunable cross-linking degrees were prepared by precisely controlling the UV dosage and subsequently terminating the cationic polymerization with methanol. Due to the sensitivity of the polymerization of diepoxies to ultraviolet irradiation dosage, precise control of the cross-linking degree can be achieved solely by regulating the irradiation time. Furthermore, cationic polymerization does not require inert atmosphere protection and can be carried out directly in air for large-scale production. Consequently, this method effectively avoids reliance on complex external fields or specialized equipment, demonstrat-

ing advantages of operational simplicity, low energy consumption, and scalability. Color patterns were observed through acetone washing and methanol swelling. These patterned films hold potential for applications in information encryption.

2. Materials and Methods

2.1. Chemical Reagents and Instruments

The syntheses and characterizations of ECHM, CA-Epoxy and Dye-1 have been reported previously [34,59,60]. Photoinitiator 1176 and co-photoinitiator ITX were purchased from Shanghai Aladdin Biochem. Techn. Co., Ltd. (Shanghai, China). Methanol, ethanol, toluene, ethyl acetate and acetone were purchased from Chinasun Specialty Products Co., Ltd. (Jiangsu, China). HDO, cyclohexanone and cyclopentanone were bought from Shanghai Macklin Biochemical Techn. Co., Ltd. (Shanghai, China). The rubbing-oriented poly(ethylene terephthalate) (PET) films were supplied by Wuxi Wanli Adhesive Material Co., Ltd. (Wuxi, China). The masks were prepared by printing the pictures on the surface of the PET films using the printer HP LaserJet P1007 (HP, Palo Alto, CA, USA). The 1D (one-dimensional) grating with 15 μm stripes was bought from Suzhou Research Materials Microtech Co., Ltd. (Suzhou, China). The period was 20 μm.

The FT-IR spectra were performed on a Nicolet 6700 spectrometer at 2.0 cm^{-1} resolution by averaging over 16 scans (NICOLET, Waltham, MA, USA). The polarized optical microscopy (POM) images were taken using a CPV-900C polarization microscope (Shanghai Optical Instrument Factory, Shanghai, China) fitted with a Linkam LTS420 hot stage (LINKAM, Tadworth, Surrey, UK). Thermogravimetric analysis (TGA) of an epoxy resin film was performed using TG/DTA 6300 (HITACHI, Tokyo, Japan). The field-emission scanning electron microscopy (FE-SEM) images were taken using a Hitachi Regulus-8230 (HITACHI, Tokyo, Japan) operating at 5.0 kV. The UV–Vis–NIR spectra were obtained with a UV–Vis spectrophotometer (UV1900i, SHIMADZU, Kyoto, Japan). The circular dichroism (CD) spectra were measured using a JASCO 815 spectrometer (JASCO, Tokyo, Japan). The HPLC-MS characterization was carried out using the UltiMate 3000 Rapid Separation (RS) HPLC Systems and the micrOTOF-Q III manufactured by Bruker Daltonic Inc. (Billerica, MA, USA). The UV LED series equipment (UVSF81T) was produced by FUTANSI Electronic Technology Co., Ltd. (Shanghai, China). The UV LED parallel light source was equipped with double aspherical quartz lenses to produce parallel light with a parallel half angle of less than 2°.

2.2. Preparation of the CLCN Films by Changing the CA-Epoxy Concentration

The preparation approach for CLCN films was as follows: An ECHM/CA-Epoxy/HDO/1176/ITX mixture was prepared at a weight ratio of 80.8/4.2/10.0/3.0/2.0, which was dissolved in a mixture of cyclohexanone/cyclopentanone (*v*/*v*, 1/4) to form a solution with 20 wt% of solid content. The solution was coated on the surface of a rubbing-oriented PET film using a 40 μm Mayer bar. After the solvents were removed at 120 °C for 3.0 min, polymerization was carried out under the irradiation of the 365 nm LED lamp (400 mW cm^{-2}) at 90 °C for 20 s. Finally, a blue CLCN film was obtained after the film was post-cured at 90 °C for about 12 h. The other CLCN films were prepared by changing the concentration of CA-Epoxy to 3.8 and 3.0 wt%, respectively.

2.3. Preparation of the CLCN Films by Terminating Cationic Polymerization with Methanol After Different 365 nm LED Lamp Irradiation Times

The preparation approach for the CLCN films was as follows: An ECHM/CA-Epoxy/HDO/1176/ITX mixture was prepared at a weight ratio of 81.2/3.8/10.0/3.0/2.0. The CLC mixture was coated on the surface of a PET film as above. Then, polymerization

was carried out under the irradiation of the 365 nm LED lamp (200 mW cm^{-2}) at 90 °C for 2.0 s. The film was immediately immersed in methanol for 5.0 min to terminate polymerization and then dried at 120 °C for 3.0 min. The other CLCN films were prepared by changing the LED lamp irradiation time and terminating with methanol after irradiation.

2.4. Preparation of the CLCN Film with the QR Code of "Epoxy Resin"

An ECHM/CA-Epoxy/HDO/1176/ITX mixture was prepared at a weight ratio of 82.0/3.0/10.0/3.0/2.0. The CLC mixture was coated on the surface of a PET film as above. Then, polymerization was carried out under the irradiation of the 365 nm LED lamp (200 mW cm^{-2}) at 90 °C for 8.0 s through the mask with the pattern of a QR code. After removing the photomask, the red CLCN film was obtained under the irradiation of the 365 nm LED lamp (200 mW cm^{-2}) for 2.0 s. The obtained red CLCN film was immediately immersed in methanol for 5.0 min to terminate polymerization. Finally, the QR code pattern was revealed by washing the film with acetone.

2.5. Preparation of the CLCN Film with the QR Code of "LC"

An ECHM/CA-Epoxy/HDO/1176/ITX mixture was prepared at a weight ratio of 81.2/3.8/10.0/3.0/2.0. The CLC mixture was coated on the surface of a PET film as above. Then, polymerization was carried out under the irradiation of the 365 nm LED lamp (200 mW cm^{-2}) at 90 °C for 9.0 s through the mask with the pattern of a QR code. After removing the photomask, the green CLCN film was obtained under the irradiation of the 365 nm LED lamp (200 mW cm^{-2}) for 1.0 s. The obtained green CLCN film was immediately immersed in methanol for 5.0 min to terminate polymerization.

2.6. Preparation of the Dye-Doped CLCN Pattern

An ECHM/CA-Epoxy/Dye-1/HDO/1176/ITX mixture was prepared at a weight ratio of 79.2/3.8/2.0/10.0/3.0/2.0. The CLC mixture was coated on the surface of a PET film as above. Then, polymerization was carried out under the irradiation of the 365 nm LED lamp (200 mW cm^{-2}) at 90 °C for 8.0 s through the mask with the pattern of a squirrel and flowers. The patterned areas were transparent, while the background was light-shielding. After removing the photomask, the green CLCN film was obtained under the irradiation of the 365 nm LED lamp (200 mW cm^{-2}) for 2.0 s. The obtained green CLCN film was immediately immersed in methanol for 5.0 min to terminate polymerization.

2.7. Preparation of the 1D CLCN Grating

The ECHM/CA-Epoxy/HDO/1176/ITX (*w*/*w*/*w*/*w*/*w*, 81.2/3.8/10.0/3.0/2.0) mixture was coated on the surface of a PET film as above. Then, polymerization was carried out under the irradiation of the 365 nm LED lamp (360 mW cm^{-2}) at 90 °C for 5.0 s through the 1D grating photomask with a period of 20 μm. After removing the photomask, the CLCN grating was obtained under the irradiation of the 365 nm LED lamp (200 mW cm^{-2}) for 2.0 s. The obtained CLCN grating was immediately immersed in methanol for 5.0 min to terminate polymerization and then dried at 120 °C for 3.0 min.

3. Results and Discussion

The diepoxy monomer ECHM exhibits nematic liquid crystalline behavior with a phase transition sequence of Tg 30.0 °C N 160.6 °C I 160.5 °C N 27.0 °C Tg (Tg, glass transition temperature; N, nematic phase; I, isotropic state) (Figure 1a) [34]. The reactive chiral dopant CA-Epoxy induces right-handed cholesteric organization [59]. Photoinitiation was achieved using 1176 and ITX as a photoinitiator/co-initiator pair. For the ECHM/CA-Epoxy/HDO/1176/ITX (*w*/*w*/*w*/*w*/*w*, 81.2/3.8/10.0/3.0/2.0) mixture, an oily streak texture was observed in the polarized optical microscopy (POM) image, indicating a

cholesteric structure (Figure S1). Moreover, the POM characterization also indicated that the clearing point of this mixture was about 113.0 °C (Figure S2). Three structural colored CLCN films were prepared by changing the CA-Epoxy concentration on the rubbing-oriented poly(ethylene terephthalate) (PET) substrate (Figure 1b). The photopolymerization was carried out under the 365 nm UV–Vis light irradiation for 20 s, and the post-polymerization was carried out at 90 °C for 12 h. It was found that the reflection bands of the CLC mixtures redshifted slightly after polymerization (Figure 1c). The selective reflection bands of the CLCN films were observed at 486, 515 and 646 nm. The polymerization of hexane-1,6-diol (HDO) was proposed to partially destroy the cholesteric structure. The optical activity of the CLCN films was characterized by circular dichroism (CD). The positions of the CD signals coincided almost exactly with those of the corresponding UV–Vis reflection bands, confirming that the colors of the CLCN films originate from selective Bragg reflection (Figure 1d). Previous results indicated that right-handed helical CLCN films could be prepared using CA-Epoxy as the chiral additive [34]. A weak negative CD signal was also observed at 368 nm, which originated from the chiral stacking of the neighboring aromatic rings. The thermal gravimetric analysis (TGA) indicated that the initial decomposition temperature of the green CLCN film was about 279 °C (Figure S3). The cross-sectional field-emission scanning electron microscopy (FE-SEM) images of the CLCN films are shown in Figure S4. The helical pitches of the CLCN films prepared using 3.0, 3.8 and 4.2 wt% of CA-Epoxy were about 361, 294 and 257 nm, respectively. According to Bragg's Law $\lambda = nP$ (where λ is the wavelength of the reflection band, n is the average refractive index, and P is the helical pitch), the decrease in helical pitch causes the selective reflection wavelength of the film to shift from approximately 646 nm to 485 nm. The observed structural color changes from red through green to blue.

To reveal the polymerization of ECHM monomers, FT-IR spectra were taken during the CLCN film preparation process (Figure 1e). For the CLC mixture with 3.8 wt% of CA-Epoxy, an absorption band was identified at 924 cm^{-1}, which originated from the epoxy group. After the CLC mixture was irradiated under the 365 nm UV light (200 mW cm^{-2}) for 2.0 s, the intensity of the absorption band decreased. After the CLCN film was post-cured at 90 °C for 12 h, the intensity decreased further, indicating that most of the ECHM molecules had been polymerized. To achieve complete conversion of epoxy groups and construct a highly cross-linked CLCN film, the irradiation time was extended to 20 s under a higher UV irradiation intensity (400 mW cm^{-2}). Under these conditions, the intensity of the absorption band corresponding to the epoxy group decreased significantly immediately after irradiation. Subsequently, after post-curing at 90 °C for 12 h, this absorption band disappeared, confirming the complete polymerization of ECHM monomers.

A series of CLCN films were prepared using the CLC mixture with the CA-Epoxy concentration of 3.8 wt% at different 365 nm UV light (200 mW cm^{-2}) irradiation times (Figure 2a). And the CLCN films were washed with acetone immediately after the irradiation. The monomers were almost totally linked to the cross-linked network after being irradiated for 20 s. Due to the low cationic polymerization rate, more non-cross-linked compounds were removed with the decrease in the irradiation time from 20 to 2.0 s. Then, the reflection band of the CLCN film shifted from 525 to 418 nm (Figure 2b). Since the number of the helix was almost kept constant after removing the non-cross-linked compounds, the content of the non-cross-linked compounds could be roughly calculated according to the equation $(\lambda_1 - \lambda_2)/\lambda_1$ (where λ_1 and λ_2 are the wavelengths of the reflection bands of the CLCN film before and after being washed with acetone, respectively). For the CLCN film prepared with an irradiation time of 2.0 s, the content of the removed compounds was about 20 wt%. Therefore, the cross-linking degree of the final CLCN film can be controlled by the UV irradiation dosage.

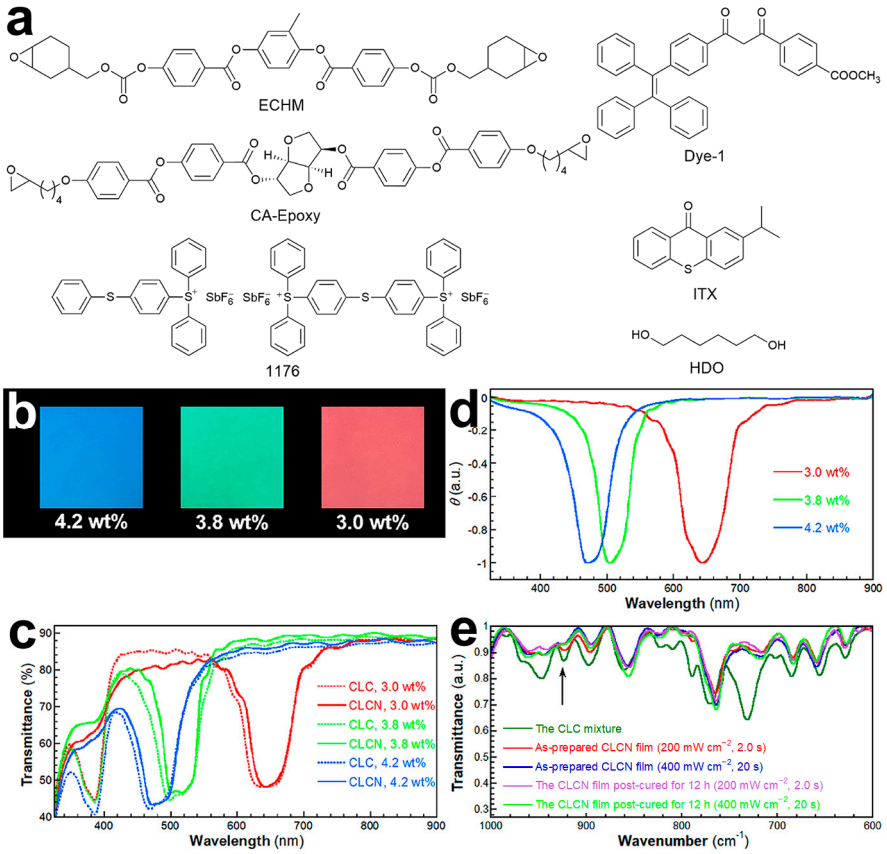


Figure 1. (**a**) Chemical structures of the compounds. (**b**) Photographs of the CLCN films and (**c**) UV–Vis–NIR spectra of the CLC mixtures and CLCN films prepared at different CA-Epoxy concentrations. (**d**) Transmission CD spectra of the CLCN films. (**e**) FT-IR spectra taken during the CLCN film preparation process.

Moreover, a series of CLCN films were prepared by terminating the polymerization using methanol after different UV light irradiation times and being dried at 120 °C for 3.0 min. Since the non-cross-linked compounds cannot be dissolved in methanol, the reflection bands of these films are almost identical (Figure 2c). To understand the termination effect of methanol, the CLCN film prepared with an irradiation time of 2.0 s was washed with acetone. The compounds dissolved in acetone were characterized using the high-performance liquid chromatography–mass spectrometer (HPLC-MS). Epoxy liquid crystal monomer derivatives bearing hydroxyl- or methoxy-substituted cyclohexyl end groups were identified at 745.2 and 759.2 $[M + Na]^+$ (Figures S5 and S6). This indicates that methanol, acting as a nucleophile, undergoes a chain transfer reaction with the active center at the growing chain terminus, forming stable terminal structures that effectively terminate cationic polymerization.

Since the polymerization of the diepoxies was sensitive to the 365 nm UV light irradiation dosage, a CLCN film was prepared by using the CLC mixture with 3.0 wt% of CA-Epoxy, shown in Figure 1c, and controlling the irradiation time at different regions (Scheme 1a and Figure 3a,b). The irradiation of the background and patterned area were 10 and 2.0 s, respectively. The polymerization was terminated using methanol. Then, a red CLCN film was obtained (Figure 3a). After the non-cross-linked compounds were removed with acetone, a green pattern with an orange background was observed (Figure 3b). Scanning the QR code displays "Epoxy Resin". This approach enabled the fabrication of CLCN films with programmable cross-linking degrees, leveraging methanol's dual functionality as both a chain transfer agent and polymerization terminator. The rapid termination kinet-

ics ensured high-fidelity pattern resolution while maintaining structural integrity of the cholesteric network.

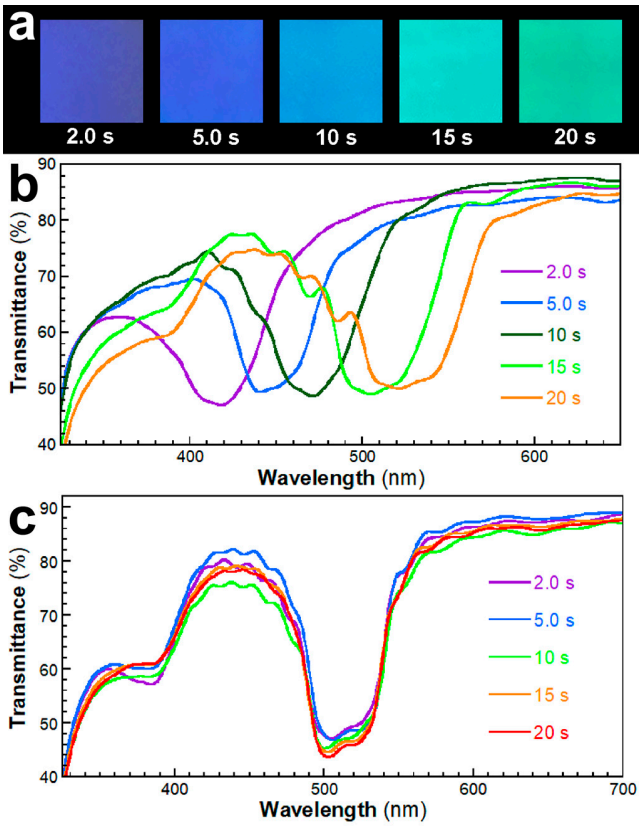
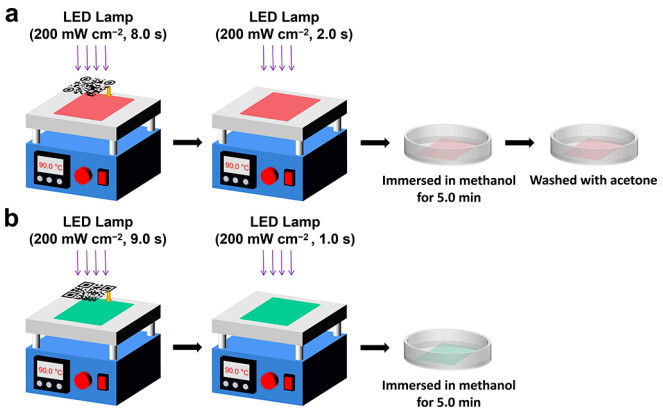


Figure 2. (**a**) Pictures and (**b**) UV–Vis spectra of the CLCN films prepared after acetone washing at different 365 nm UV light irradiation times; (**c**) UV–Vis spectra of CLCN films prepared after methanol treatment at different 365 nm UV light irradiation times.



Scheme 1. Schematic representation of the preparation processes of the CLCN patterns by (**a**) washing with acetone and (**b**) treating with methanol.

A patterned CLCN film was prepared using the CLC mixture with 3.8 wt% of CA-Epoxy, shown in Figure 1c. The irradiation times of the background and patterned area were 10 and 1.0 s, respectively. The preparation procedure is illustrated in Scheme 1b. Based on the regional photopolymerization methodology, we also quenched the cationic active centers using methanol. After immersing the film in methanol for 5.0 min to terminate cationic polymerization and subsequently evaporating the solvent, a green CLCN film containing two regions with different cross-linking densities was observed in air (Figure 3c). Namely, both of these regions exhibited a green structural color. After the dried film was

immersed in methanol for just 90 s, a red pattern with a green background was observed (Figure 3d). Scanning the QR code displays "LC". Upon re-evaporation of the methanol, only the green structural color was observed again. Therefore, this pattern can be applied for encryption. A 1D CLCN grating with a period of 20 μm was also prepared using this CLC mixture and a photomask. The POM image taken in reflection mode indicates a high resolution (Figure S7). Moreover, defects were also observed at the film surface, which could result from the high polymerization rate [61].

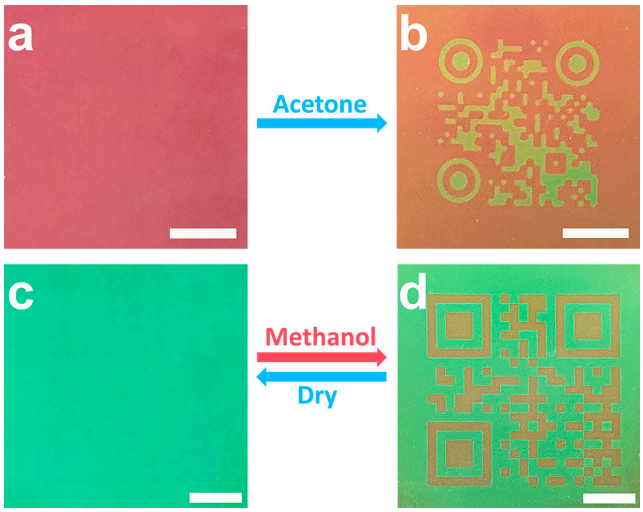


Figure 3. Photographs of the CLCN film taken (**a**) before and (**b**) after washing with acetone. "Epoxy Resin" was observed after being scanned. Photographs of the CLCN film taken in (**c**) air and (**d**) methanol. "LC" was observed after being scanned (scale bar: 1.0 cm).

To evaluate the durability and environmental stability required for CLCN films in practical encryption applications, a film was prepared using the same CLC mixture. After irradiation with the 365 nm UV light for 2.0 s, the cationic polymerization reaction was quenched with methanol. A series of tests were then conducted on this film. First, the cycling stability of this CLCN film under cyclic conditions was investigated. Immersion in methanol resulted in a shift in the selective Bragg reflection band from 514 to 568 nm. Through ten cycles of immersion in methanol and removal, the wavelength of the Bragg reflection band remained stable in both dry and swollen states (Figure S8). This demonstrates the excellent reversibility and fatigue resistance of the encryption–decryption function. Since this swelling increases the helical pitch, the volume ratio of methanol within the swelled film can be roughly calculated to be 10 wt%, based on the equation $(\lambda_1 - \lambda_2)/\lambda_1$ (where λ_1 and λ_2 are the wavelengths of the reflection bands of the CLCN film after and before being immersed in methanol, respectively).

Second, the long-term thermal stability was assessed via accelerated thermal aging at 120 °C for 24 h. After heat treatment, the reflection band of the dry film blue-shifted to 505 nm, representing a 9 nm change from the initial 514 nm (Figure S9). This minor shift may result from minor irreversible shrinkage of the polymer network at elevated temperature. Notably, the thermally treated film retained its ability to swell in methanol, shifting its reflection band to 562 nm. The swelling-induced wavelength shift of 57 nm was comparable to the 54 nm shift observed for the pristine film in Figure S8. This result indicates that the thermal aging process did not affect the swelling capacity of the CLCN. Finally, to assess the practical application potential of this film, its stability in common solvents was investigated. As shown in Figure S10, after immersing the film in water, ethanol, toluene, and ethyl acetate for 8.0 min, no significant band shifts were observed.

This result confirms the excellent stability of the CLCN film against common solvents. This film can also be applied for the discrimination of methanol and ethanol [36].

The luminescence phenomenon in aggregation-induced emission (AIE) materials is typically attributed to the restriction of intramolecular motions (RIMs) [62]. Taking the iconic AIE chromophore tetraphenylethene (TPE) as an example, in dilute solutions, the rotation of the phenyl groups results in weak fluorescence or complete quenching [63,64]. Conversely, in the aggregated state, intramolecular rotation of the aryl rotors becomes greatly restricted, thereby opening up the radiative channel [65]. Here, a TPE derivative, Dye-1, was employed [60]. Under the excitation of 380 nm UV light, Dye-1 emits green light in the solid state. A dye-doped colorful film was prepared using the ECHM/CA-Epoxy/Dye-1/HDO/1176/ITX (*w*/*w*/*w*/*w*/*w*/*w*, 79.2/3.8/2.0/10.0/3.0/2.0) mixture and a photomask, and methanol was used for the cationic polymerization termination (Figure 4a). The background and patterned area were irradiated under the 365 nm UV light (200 mW cm^{-2}) for 2.0 s and 10 s, respectively. Due to the RIM of Dye-1, the pattern was observed under the irradiation of the 365 nm UV light (Figure 4b). The green emission intensity of the patterned area was higher than that of the background area (Figure 5). Therefore, the pattern shown here could potentially be applied to decorations and anti-counterfeiting.

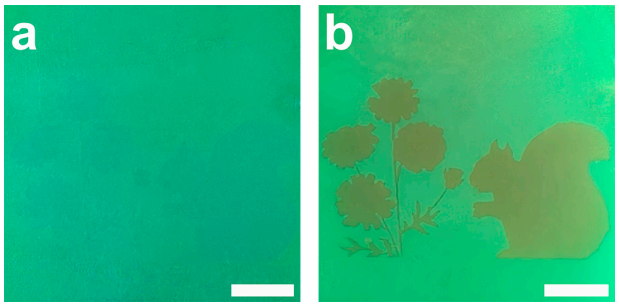


Figure 4. Photographs of the dye-doped CLCN pattern taken under (**a**) natural and (**b**) 365 nm UV lights (scale bar: 1.0 cm).

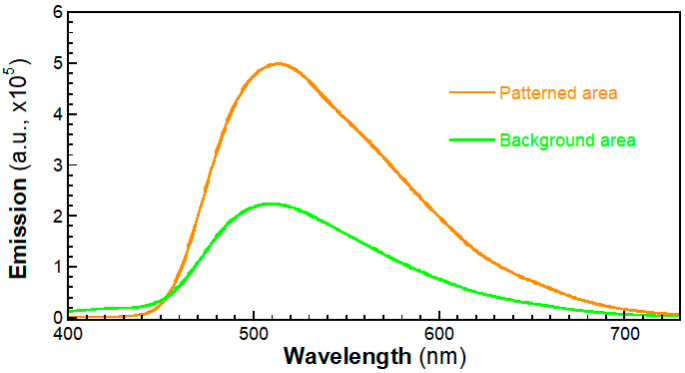


Figure 5. Emission spectra of the dye-doped film from the background and patterned areas (λ_{ex} = 380 nm).

4. Conclusions

Structural colored CLCN films were prepared using an epoxy liquid crystal monomer and a chiral dopant through cationic photopolymerization. Due to the low rate of cationic polymerization, the cross-linking degree of the CLCN films was controlled by changing the UV light irradiation dosage and using methanol to terminate the polymerization reaction. The reflection band of the CLCN film can be changed by removing the unpolymerized compounds using acetone or by swelling the film with methanol. Based on this, structural colored epoxy resin films were prepared using photomasks. After acetone washing, stable visible patterns were formed, while methanol swelling enabled dynamic reversible pattern

visualization. This encryption strategy enables information encryption and decryption through simple solvent treatment. Due to the oxygen insensitivity of cationic photopolymerization, these patterned films can be mass-prepared on coating lines, demonstrating potential application value in the field of information encryption.

Supplementary Materials: The following supporting information can be downloaded at https://www.mdpi.com/article/10.3390/chemistry8020024/s1, Figure S1: POM image of the ECHM/CA-Epoxy/HDO/1176/ITX (*w*/*w*/*w*/*w*/*w*, 81.2/3.8/10.0/3.0/2.0) mixture taken at 90.0 °C during the cooling process; Figure S2: POM image of the ECHM/CA-Epoxy/HDO/1176/ITX (*w*/*w*/*w*/*w*/*w*, 81.2/3.8/10.0/3.0/2.0) mixture taken at 113.0 °C during the heating process; Figure S3: TGA curve of the CLCN film; Figure S4: Cross-sectional FE-SEM images of the CLCN films prepared at the CA-Epoxy concentrations of (a) 3.0 wt%, (b) 3.8 wt% and (c) 4.2 wt%; Figure S5: Chemical structures of partial chemicals dissolved in acetone; Figure S6: HPLC-MS curves and spectra of the chemicals dissolved in acetone; Figure S7: POM image of the 1D CLCN grating taken in reflection mode; Figure S8: λ_{max} values of the CLCN film after being immersed in methanol and dried in air ten times; Figure S9: UV–Vis spectra of the thermally aged CLCN film in the dry state and the methanol-swollen state; Figure S10: UV–Vis spectra of the CLCN film in the dry state and in different solvents.

Author Contributions: Conceptualization, Y.Y. (Yonggang Yang); investigation, Y.Y. (Yingying Yi) and W.Y.; writing—original draft preparation, Y.Y. (Yingying Yi), Y.L. and W.L.; writing—review and editing, W.L. and Y.Y. (Yonggang Yang); supervision, Y.Y. (Yonggang Yang); project administration, Y.L. and Y.Y. (Yonggang Yang); funding acquisition, Y.Y. (Yonggang Yang). All authors have read and agreed to the published version of the manuscript.

Funding: This work was supported by the National Natural Science Foundation of China (52273212), Jiangsu Engineering Laboratory of Novel Functional Polymeric Materials, Jiangsu Key Laboratory of Advanced Functional Polymer Materials, and the Key Laboratory of Polymeric Materials Design and Synthesis for Biomedical Function.

Data Availability Statement: The original contributions presented in the study are included in the article/Supplementary Materials, and further inquiries can be directed to the corresponding author.

Conflicts of Interest: The authors declare no conflicts of interest.

References

1. Bisoyi, H.K.; Bunning, T.J.; Li, Q. Stimuli-Driven Control of the Helical Axis of Self-Organized Soft Helical Superstructures. *Adv. Mater.* **2018**, *30*, 1706512. [CrossRef]
2. Zhang, P.; de Haan, L.T.; Debije, M.G.; Schenning, A.P.H.J. Liquid Crystal-Based Structural Color Actuators. *Light Sci. Appl.* **2022**, *11*, 248. [CrossRef]
3. Tran, A.; Boott, C.E.; MacLachlan, M.J. Understanding the Self-Assembly of Cellulose Nanocrystals—Toward Chiral Photonic Materials. *Adv. Mater.* **2020**, *32*, 1905876. [CrossRef]
4. Wang, Y.; Li, Q. Light-Driven Chiral Molecular Switches or Motors in Liquid Crystals. *Adv. Mater.* **2012**, *24*, 1926–1945. [CrossRef]
5. Mitov, M. Cholesteric Liquid Crystals with a Broad Light Reflection Band. *Adv. Mater.* **2012**, *24*, 6260–6276. [CrossRef]
6. Lan, R.; Shen, W.; Yao, W.; Chen, J.; Chen, X.; Yang, H. Bioinspired Humidity-Responsive Liquid Crystalline Materials: From Adaptive Soft Actuators to Visualized Sensors and Detectors. *Mater. Horiz.* **2023**, *10*, 2824–2844. [CrossRef]
7. Ko, H.; Kim, M.; Wi, Y.; Rim, M.; Lim, S.-I.; Koo, J.; Kang, D.-G.; Jeong, K.-U. Chiroptical Smart Paints: Polymerization of Helical Structures in Cholesteric Liquid Crystal Films. *J. Chem. Educ.* **2021**, *98*, 2649–2654. [CrossRef]
8. Zhang, X.; Dong, Y.; Chen, Y.; Liu, Y. High Humidity Responsive Cholesteric Liquid Crystal Polymer Film for Anti-Counterfeiting Encryption Applications. *Opt. Mater.* **2025**, *168*, 117461. [CrossRef]
9. Zhang, W.; Guan, P.; Zhao, J.; Yang, Y.; Li, H. Circularly Polarized Room-Temperature Phosphorescence from Dye-Doped Cholesteric Liquid Crystalline Polymer Networks. *J. Phys. Chem. Lett.* **2025**, *16*, 725–730. [CrossRef] [PubMed]
10. Guan, P.; Shi, F.; Xu, C.; Yang, Y.; Li, H. Tunable Circularly Polarized Afterglow from Cholesteric Liquid Crystalline Polymer Networks. *J. Phys. Chem. Lett.* **2025**, *16*, 10142–10148. [CrossRef] [PubMed]
11. Bao, J.; Wang, Z.; Shen, C.; Huang, R.; Song, C.; Li, Z.; Hu, W.; Lan, R.; Zhang, L.; Yang, H. Freestanding Helical Nanostructured Chiro-Photonic Crystal Film and Anticounterfeiting Label Enabled by a Cholesterol-Grafted Light-Driven Molecular Motor. *Small Methods* **2022**, *6*, 2200269. [CrossRef] [PubMed]

12. Kragt, A.J.J.; Zuurbier, N.C.M.; Broer, D.J.; Schenning, A.P.H.J. Temperature-Responsive, Multicolor-Changing Photonic Polymers. *ACS Appl. Mater. Interfaces* **2019**, *11*, 28172–28179. [CrossRef] [PubMed]
13. Zhang, J.; Zhang, S.; Liu, J.; Ren, Y.; Chen, J.; Hu, W.; Yang, H. Simultaneous or Independent Programming and Reconfiguration of Structural and Fluorescent Information in Multi-Stimuli-Responsive Liquid Crystalline Polymer Film. *Chem. Eng. J.* **2025**, *505*, 159583. [CrossRef]
14. Kragt, A.J.J.; Hoekstra, D.C.; Stallinga, S.; Broer, D.J.; Schenning, A.P.H.J. 3D Helix Engineering in Chiral Photonic Materials. *Adv. Mater.* **2019**, *31*, 1903120. [CrossRef]
15. Zhang, P.; Kragt, A.J.J.; Schenning, A.P.H.J.; de Haan, L.T.; Zhou, G. An Easily Coatable Temperature Responsive Cholesteric Liquid Crystal Oligomer for Making Structural Colour Patterns. *J. Mater. Chem. C* **2018**, *6*, 7184–7187. [CrossRef]
16. Feng, W.; Pal, A.; Wang, T.; Ren, Z.; Yan, Y.; Lu, Y.; Yang, H.; Sitti, M. Cholesteric Liquid Crystal Polymeric Coatings for Colorful Artificial Muscles and Motile Humidity Sensor Skin Integrated with Magnetic Composites. *Adv. Funct. Mater.* **2023**, *33*, 2300731. [CrossRef]
17. Moirangthem, M.; Arts, R.; Merkx, M.; Schenning, A.P.H.J. An Optical Sensor Based on a Photonic Polymer Film to Detect Calcium in Serum. *Adv. Funct. Mater.* **2016**, *26*, 1154–1160. [CrossRef]
18. Zhang, P.; Shi, X.; Schenning, A.P.H.J.; Zhou, G.; de Haan, L.T. A Patterned Mechanochromic Photonic Polymer for Reversible Image Reveal. *Adv. Mater. Interfaces* **2020**, *7*, 1901878. [CrossRef]
19. Brannum, M.T.; Steele, A.M.; Venetos, M.C.; Korley, L.T.J.; Wnek, G.E.; White, T.J. Light Control with Liquid Crystalline Elastomers. *Adv. Opt. Mater.* **2019**, *7*, 1801683. [CrossRef]
20. Herzer, N.; Guneysu, H.; Davies, D.J.D.; Yildirim, D.; Vaccaro, A.R.; Broer, D.J.; Bastiaansen, C.W.M.; Schenning, A.P.H.J. Printable Optical Sensors Based on H-Bonded Supramolecular Cholesteric Liquid Crystal Networks. *J. Am. Chem. Soc.* **2012**, *134*, 7608–7611. [CrossRef]
21. Chang, C.-K.; Bastiaansen, C.W.M.; Broer, D.J.; Kuo, H.L. Discrimination of Alcohol Molecules Using Hydrogen-Bridged Cholesteric Polymer Networks. *Macromolecules* **2012**, *45*, 4550–4555. [CrossRef]
22. Yang, Y.; Zhou, D.; Liu, X.; Liu, Y.; Liu, S.; Miao, P.; Shi, Y.; Sun, W. Optical Fiber Sensor Based on a Cholesteric Liquid Crystal Film for Mixed Voc Sensing. *Opt. Express* **2020**, *28*, 31872–31881. [CrossRef]
23. McConney, M.E.; Tondiglia, V.P.; Hurtubise, J.M.; Natarajan, L.V.; White, T.J.; Bunning, T.J. Thermally Induced, Multicolored Hyper-Reflective Cholesteric Liquid Crystals. *Adv. Mater.* **2011**, *23*, 1453–1457. [CrossRef]
24. Kragt, A.J.J.; Broer, D.J.; Schenning, A.P.H.J. Easily Processable and Programmable Responsive Semi-Interpenetrating Liquid Crystalline Polymer Network Coatings with Changing Reflectivities and Surface Topographies. *Adv. Funct. Mater.* **2018**, *28*, 1704756. [CrossRef]
25. Miao, Z.; Chen, X.; Zhang, Y.; Wang, D.; Wang, L. Bistable Cholesteric Liquid Crystal Films with Excellent Electro-Optical Performance and Spacing Stability for Reflective Displays. *ACS Appl. Polym. Mater.* **2023**, *5*, 476–484. [CrossRef]
26. Yagci, Y.; Jockusch, S.; Turro, N.J. Photoinitiated Polymerization: Advances, Challenges, and Opportunities. *Macromolecules* **2010**, *43*, 6245–6260. [CrossRef]
27. Noè, C.; Malburet, S.; Bouvet-Marchand, A.; Graillot, A.; Loubat, C.; Sangermano, M. Cationic Photopolymerization of Bio-Renewable Epoxidized Monomers. *Prog. Org. Coat.* **2019**, *133*, 131–138. [CrossRef]
28. Auvergne, R.; Caillol, S.; David, G.; Boutevin, B.; Pascault, J.-P. Biobased Thermosetting Epoxy: Present and Future. *Chem. Rev.* **2014**, *114*, 1082–1115. [CrossRef]
29. Abad, M.; Martínez-Bueno, A.; Concellón, A. Shaping Liquid Crystal Polymer Networks: From Molecular Design and Processing to Multifunctional Materials. *Adv. Mater. Technol.* **2025**, *10*, e01236. [CrossRef]
30. Fu, C.; Li, D.; Liu, C.; Zhang, Y.; Zhang, J.; Cheng, Y. Chiral Co-Assembled Liquid Crystal Polymer Network Enabled by In-Situ Photopolymerization for High-Performance CP-OLEDs. *Angew. Chem. Int. Ed.* **2025**, *64*, e202512257. [CrossRef]
31. Park, J.; Yu, T.; Inagaki, T.; Akagi, K. Helical Network Polymers Exhibiting Circularly Polarized Luminescence with Thermal Stability. Synthesis via Photo-Cross-Link Polymerizations of Methacrylate Derivatives in a Chiral Nematic Liquid Crystal. *Macromolecules* **2015**, *48*, 1930–1940. [CrossRef]
32. Pu, Y.; Wen, X.; Gu, H.; Zhu, H.; Yuan, M.; Huang, J.; Zhan, Q.; Jiang, X.-F.; Polavarapu, L.; Hu, X.; et al. Upconversion Circularly Polarized Luminescence with Dissymmetry Factor up to 1.80 from Flexible Perovskite-Liquid Crystal Membranes. *Chem. Eng. J.* **2025**, *512*, 162515. [CrossRef]
33. Ma, J.; Yang, Y.; Valenzuela, C.; Zhang, X.; Wang, L.; Feng, W. Mechanochromic, Shape-Programmable and Self-Healable Cholesteric Liquid Crystal Elastomers Enabled by Dynamic Covalent Boronic Ester Bonds. *Angew. Chem. Int. Ed.* **2022**, *61*, e202116219. [CrossRef]
34. Yi, Y.; Yang, W.; Li, Y.; Liu, W.; Yang, Y. Colorful Patterns Prepared Using Alicyclic Epoxy-Based Cholesteric Liquid Crystal Inks for Decoration. *Liq. Cryst.* **2025**, *52*, 434–444. [CrossRef]
35. Zhang, X.; Guo, Y.; Li, Y.; Liu, W.; Li, H.; Yang, Y. Colorfully Patterned Epoxy Resin Films with a Cholesteric Structure Prepared through a Photopolymerization Approach. *ACS Appl. Polym. Mater.* **2023**, *5*, 193–200. [CrossRef]

36. Guo, Y.; Yi, Y.; Wu, L.; Liu, W.; Li, Y.; Yang, Y. A Structural Colored Epoxy Resin Sensor for the Discrimination of Methanol and Ethanol. *Chemistry* **2025**, *7*, 122. [CrossRef]
37. Chen, Z.; Chen, Y.; Guo, Y.; Yang, Z.; Li, H.; Liu, H. Paper-Structure Inspired Multiresponsive Hydrogels with Solvent-Induced Reversible Information Recording, Self-Encryption, and Multidecryption. *Adv. Funct. Mater.* **2022**, *32*, 2201009. [CrossRef]
38. Sang, J.; Lv, Z.; Li, T.; Chen, F.; Li, H.; Yang, B.; Sun, J.; Shang, J.; Zheng, J. Flexible and Wearable Dual-Channel Liquid Crystal Polymer Film for High-Performance Security Information Encryption. *Opt. Express* **2025**, *33*, 25718–25727. [CrossRef] [PubMed]
39. He, Q.; Zhao, Q.; Zhang, L. Long-Chain Crosslinker-Induced Patterning on an Elastic Polymer Film for Robust and Reversible Information Encryption/Decryption. *Mater. Horiz.* **2025**, *12*, 2360–2368. [CrossRef]
40. Ren, X.; Liu, Z.; Zhang, Q.; Cheng, R.; Yin, D.; Ge, F.; Zhang, Q. Carbon Black-Containing Cholesteric Liquid Crystal Elastomers Enabling Multi-Level Information Encryption and Multimode Actuation. *Adv. Funct. Mater.* **2025**, *36*, e17597. [CrossRef]
41. Zhang, X.; Zhong, Z.; Lu, Y.; Yang, D.; Li, Y.; Zhao, Y.; He, Z.; Luan, Y. Cholesterol Liquid Crystals with Thermoelectric Stimulation for Multi-Decryption Condition-Dependent Digital Information Encryption and Visible Light Camouflage. *Chem. Eng. J.* **2025**, *525*, 170212. [CrossRef]
42. Michaudel, Q.; Kottisch, V.; Fors, B.P. Cationic Polymerization: From Photoinitiation to Photocontrol. *Angew. Chem. Int. Ed.* **2017**, *56*, 9670–9679. [CrossRef] [PubMed]
43. Pierau, L.; Elian, C.; Akimoto, J.; Ito, Y.; Caillol, S.; Versace, D.-L. Bio-Sourced Monomers and Cationic Photopolymerization–the Green Combination Towards Eco-Friendly and Non-Toxic Materials. *Prog. Polym. Sci.* **2022**, *127*, 101517. [CrossRef]
44. Park, S.; Kilgallon, L.J.; Yang, Z.; Ryu, D.Y.; Ryu, C.Y. Molecular Origin of the Induction Period in Photoinitiated Cationic Polymerization of Epoxies and Oxetanes. *Macromolecules* **2019**, *52*, 1158–1165. [CrossRef]
45. Kepkow, M.; Heinz, M.; Strehmel, B.; Strehmel, V. Synthesis and Photoinitiated Cationic Polymerization of Epoxy Monomers Derived from Oleic Acid Comprising One to Three Epoxy Groups. *Sustain. Chem. Pharm.* **2024**, *39*, 101588. [CrossRef]
46. Liao, F.-Q.; Chen, Y.-C. Siloxane-Based Epoxy Coatings through Cationic Photopolymerization for Corrosion Protection. *Prog. Org. Coat.* **2023**, *174*, 107235. [CrossRef]
47. Jellali, R.; Campistron, I.; Laguerre, A.; Lecamp, L.; Pasetto, P.; Bunel, C.; Mouget, J.-L.; Pilard, J.-F. Synthesis and Crosslinking Kinetic Study of Epoxidized and Acrylated/Epoxidized Oligoisoprenes: Comparison between Cationic and Radical Photopolymerization. *J. Appl. Polym. Sci.* **2013**, *128*, 2489–2497. [CrossRef]
48. Ficek, B.A.; Thiesen, A.M.; Scranton, A.B. Cationic Photopolymerizations of Thick Polymer Systems: Active Center Lifetime and Mobility. *Eur. Polym. J.* **2008**, *44*, 98–105. [CrossRef]
49. Frison, T.; Irlweg, A.; Ergül, Ö.; Totev, D.I.; Tuinier, R.; Esteves, A.C.C. Electron Beam-Induced Cationic Polymerization Drives Structure and Properties of Epoxy Coatings. *Prog. Org. Coat.* **2025**, *200*, 109017. [CrossRef]
50. Kaalberg, S.; Jessop, J.L.P. Enhancing Cationic Ring-Opening Photopolymerization of Cycloaliphatic Epoxides Via Dark Cure and Oxetanes. *J. Polym. Sci. A Polym. Chem.* **2018**, *56*, 1436–1445. [CrossRef]
51. Malik, M.S.; Schlögl, S.; Wolfahrt, M.; Sangermano, M. Review on UV-Induced Cationic Frontal Polymerization of Epoxy Monomers. *Polymers* **2020**, *12*, 2146. [CrossRef]
52. Bednarczyk, P.; Irska, I.; Gziut, K.; Ossowicz-Rupniewska, P. Synthesis of Epoxy Methacrylate Resin and Coatings Preparation by Cationic and Radical Photocrosslinking. *Molecules* **2021**, *26*, 7663. [CrossRef] [PubMed]
53. Sangermano, M.; Razza, N.; Crivello, J.V. Cationic UV-Curing: Technology and Applications. *Macromol. Mater. Eng.* **2014**, *299*, 775–793. [CrossRef]
54. Škola, O.; Jašúrek, B.; Veselý, D.; Němec, P. Mechanical Properties of Polymer Layers Fabricated Via Hybrid Free Radical-Cationic Polymerization of Acrylate, Epoxide, and Oxetane Binders. *Prog. Org. Coat.* **2016**, *101*, 279–287. [CrossRef]
55. Hartwig, A.; Koschek, K.; Lühring, A.; Schorsch, O. Cationic Polymerization of a Cycloaliphatic Diepoxide with Latent Initiators in the Presence of Structurally Different Diols. *Polymer* **2003**, *44*, 2853–2858. [CrossRef]
56. Dillman, B.; Jessop, J.L.P. Chain Transfer Agents in Cationic Photopolymerization of a Bis-Cycloaliphatic Epoxide Monomer: Kinetic and Physical Property Effects. *J. Polym. Sci. A Polym. Chem.* **2013**, *51*, 2058–2067. [CrossRef]
57. Li, S.; He, Y.; Nie, J. Photopolymerization of Hybrid Monomer 3-(1-Propenyl)Oxypropyl Acrylate. *J. Photochem. Photobiol. A Chem.* **2007**, *191*, 25–31. [CrossRef]
58. Olsson, R.T.; Bair, H.E.; Kuck, V.; Hale, A. Acceleration of the Cationic Polymerization of an Epoxy with Hexanediol. *J. Therm. Anal. Calorim.* **2004**, *76*, 367–377. [CrossRef]
59. Guo, Y.; Zhao, J.; Wu, L.; Liu, W.; Li, Y.; Yang, Y. Control the Structure of the Polyacrylate/Epoxy Resin Film through Photopolymerisation. *Liq. Cryst.* **2024**, *51*, 223–232. [CrossRef]
60. Yang, H.; Zhang, W.; Lu, X.; Liu, W.; Wang, Y.; Li, H.; Yang, Y. Tetraphenylethene-Decorated Difluoroboron β-Diketonates with Terminal Chiral α-Phenylethylamine: Aggregation-Induced Emission, Circularly Polarized Luminescence and Mechanofluochromism. *Dyes Pigm.* **2021**, *192*, 109396. [CrossRef]
61. Guo, Y.; Zhao, J.; Li, Y.; Liu, W.; Yang, Y. Preparation and Application of the Epoxy Resin-based Polymer-stabilised Cholesteric Liquid Crystal Films with microcracks at the Surface. *Liq. Cryst.* **2023**, *50*, 2047–2058. [CrossRef]

62. Zhou, J.; Chang, Z.; Jiang, Y.; He, B.; Du, M.; Lu, P.; Hong, Y.; Kwok, H.S.; Qin, A.; Qiu, H.; et al. From Tetraphenylethene to Tetranaphthylethene: Structural Evolution in Aie Luminogen Continues. *Chem. Commun.* **2013**, *49*, 2491–2493. [CrossRef]
63. Shustova, N.B.; McCarthy, B.D.; Dincă, M. Turn-On Fluorescence in Tetraphenylethylene-Based Metal–Organic Frameworks: An Alternative to Aggregation-Induced Emission. *J. Am. Chem. Soc.* **2011**, *133*, 20126–20129. [CrossRef]
64. Dong, Y.; Lam, J.W.Y.; Qin, A.; Liu, J.; Li, Z.; Tang, B.Z.; Sun, J.; Kwok, H.S. Aggregation-Induced Emissions of Tetraphenylethene Derivatives and Their Utilities as Chemical Vapor Sensors and in Organic Light-Emitting Diodes. *Appl. Phys. Lett.* **2007**, *91*, 011111. [CrossRef]
65. Iasilli, G.; Battisti, A.; Tantussi, F.; Fuso, F.; Allegrini, M.; Ruggeri, G.; Pucci, A. Aggregation-Induced Emission of Tetraphenylethylene in Styrene-Based Polymers. *Macromol. Chem. Phys.* **2014**, *215*, 499–506. [CrossRef]

Disclaimer/Publisher's Note: The statements, opinions and data contained in all publications are solely those of the individual author(s) and contributor(s) and not of MDPI and/or the editor(s). MDPI and/or the editor(s) disclaim responsibility for any injury to people or property resulting from any ideas, methods, instructions or products referred to in the content.